Structural characterization of water-soluble polysaccharides from Nitraria retusa fruits and their antioxidant and hypolipidemic activities

Ilhem Rjeibi, Anouar Feriani, Faiez Hentati, Najla Hfaiedh, Philippe Michaud, Guillaume Pierre

Structural characterization of water-soluble polysaccharides from *Nitraria retusa* fruits and their antioxidant and hypolipidemic activities

Ilhem Rjeibi[a], Anouar Feriani[a], Faiez Hentati[b,c], Najla Hfaiedh[a], Philippe Michaud[c], Guillaume Pierre[c,*]

[a] Research unit of Macromolecular Biochemistry and Genetics, Faculty of Sciences of Gafsa, 2112 Gafsa, Tunisia.

[b] Unité de Biotechnologie des Algues, Biological Engineering Department, National School of Engineers of Sfax, University of Sfax, Sfax, Tunisia.

[c] Université Clermont Auvergne, CNRS, SIGMA Clermont, Institut Pascal, F-63000 Clermont-Ferrand, France.

* Corresponding author.

E-mail address: guillaume.pierre@uca.fr (G. Pierre).

Abstract: The structure, antioxidant and anti-hyperlipidemic activities of polysaccharides from *Nitraria retusa* fruits (named as NRFP) were investigated. The NRFP fraction, with a molecular weight of 66.5 kDa, was composed of a *β*-(1→3)-glucan, containing neutral sugars (69.1%) but also uronic acids up to 23.1% due to pectin structure. The monosaccharide composition highlighted a polymer composed of glucose (41.4%), galacturonic acid (30.5%), galactose (12.6%), arabinose (11.8%) and rhamnose (3.70%). In the antioxidant assays, NRFP exhibited effective total antioxidant capacity (IC_{50} = 7.82 mg/mL), scavenging activities on DPPH radical (IC_{50} = 0.87 mg/mL) and hydrogen peroxide (IC_{50} = 2.03 mg/mL). In addition, NRFP proved protective effects on H_2O_2 induced hemolysis (IC_{50} = 66.2 µg/mL). *In vivo* NRFP reduced the hyperlipidemia, hepatotoxicity, cardiovascular and coronary diseases induced by Triton X-100.

Keywords: *Nitraria retusa*; *β*-(1,3)-glucan; Pectin; Biological activities.

1. Introduction

Plant polysaccharides are natural polymers certified as nontoxic, biodegradable and do not induce any side effects. In recent years, they have attracted wide attention owing to their multiple functional properties, *e.g.*, emulsifying, foaming, water-holding and oil-holding capacities [1]. Polysaccharides have many biological activities, including anti-inflammatory and hepatoprotective effects [2,3], antioxidant and antimicrobial properties [4], but also antitumor and immunomodulatory activities [5]. Another beneficial effect of natural polysaccharides is the ability to scavenge free radicals, such as hydroxyl radicals, ABTS (2,2'-azino-bis(3-ethylbenzothiazoline-6-sulphonic acid)), DPPH (2,2-diphenyl-1-picrylhydrazyl) and superoxide radicals. In fact, natural polymers play a crucial role in defending against oxidative stress in human organisms and protect against associated diseases like neurological, cardiovascular, asthma and diabetes diseases [6]. In addition, several researchers have reported that polysaccharides have anti-nociceptive effects and reduce leukocyte migration and cytokine amounts (TNF-α and IL-8) [7,8]. Few studies have also reported that natural polysaccharides exhibit potential anti-hyperlipidemic activities *in vivo* [9,10].

Hyperlipidemia described as hypercholesterolemia is the key risk factors that intensify and accelerate the progression of atherosclerotic lesions and the development of cardiovascular disease, which are the most common causes of death in the developed world [11]. Accordingly, treatment of hyperlipidemia can mitigate the risk of the occurrence of these diseases. Moreover, previous studies have demonstrated the role of reactive oxygen species in the complications of hypercholesterolemia [9,10,12]. This pathology can be treatable by cholesterol-lowering therapies. However, the use of synthetic drugs (niacin, statin and fibrate) is frequently linked to various side effects, essentially the inflammation of the liver, adnominal skin rashes and constipation [13]. Hence, given their important exploration as functional and safe bioactive

constituents, carbohydrates from plant sources can be screened as new drugs for preventing hypercholesterolemia and related complications.

The genus *Nitraria* of the family Nitrariaceae comprises 13 species that are distributed in the northwest province of China, Europe, Australia, Asia, and Africa. These plants have wide application in traditional medicine and have been used for the treatment of diverse diseases, such as hypertension for *N. sibirica* [14], anti-arrhythmic for *N. tangutorum* [15] and antispasmodic for *N. schoberi* [16]. Recent scientific studies have demonstrated the hypolipidemic effect of anthocyanins from the fruits of *N. tangutorun* [17].

Nitraria retusa is a resistant shrub plant, widespread in Tunisia, Saudi Arabia, Egypt, Jordan and Algeria. In Tunisia, it is popularly known as Ghardaq. Leaves infusion are used to treat manifold inflammatory states and wounds [18]. The ethnopharmacological studies have demonstrated that *N. retusa* possesses multiple biological activities, mainly anti-proliferative and antioxidant properties [19], anti-microbial and anti-obesity effects [20,21] and hepato-nephroprotective activities [22, 23]. The pharmacological properties attributed to *N. retusa* are assigned to variety of compounds, such as alkaloids, flavonoids (isorhamnetin) and essential oils [19,24,25]. Despite all these reports on the phytochemical and therapeutic effects of *N. retusa*, none information is available about the characterization of its polysaccharides and associated biological activities. Thus, this paper deals with the structural analysis of a water-soluble polysaccharide (NRFP) extracted from the fruits of *N. retusa*. Various biological properties were also investigated, i.e. *in vitro* antioxidant activities, *in vivo* hepatoprotective, *in vivo* cardioprotective and *in vivo* hypolipidemic properties in mice model.

2. Materials and methods

2.1. Plant material and chemicals

Nitraria retusa fruits were sampled from Tabeddit, Gafsa (34°25'60" N latitude and 8°16'0"E longitude), in November 2016, identified and deposited at the herbarium in the Faculty of

Sciences Gafsa, Tunisia. The fruits were washed with cold water, dried under shade, grounded to a fine powder (< 50 mesh) and stored at room temperature until further uses. All chemicals were from Sigma-Aldrich and of analytical grade.

2.2. Extraction and purification of NRFP from *N. retusa* fruits

N. retusa fruits powder was at first extracted using ethanol (95%) to remove pigments, then extracted using hot water for 2 h at 100°C. After centrifugation at 5000 rpm for 20 min using a refrigerated centrifuge (Thermo Jouan GR4i, Germany), the supernatant was precipitated overnight at 4°C by adding cold anhydrous ethanol (95%). The crude polysaccharide (CP) obtained after a new centrifugation (4500 rpm, 15 min, 4°C) was deproteinized by Sevag method. Briefly, CP was dissolved in distilled water and extracted with four volumes of chloroform and one volume of n-butanol. The obtained aqueous fraction was dialyzed against double-distilled water for three days. The solution was then adjusted to 80% concentration using ethanol and conserved at 4°C for 24 h. After centrifugation (4500 rpm, 20 min, 4°C), the precipitate was suspended in distilled water and freeze dried to obtain the polysaccharide fraction called NRFP.

2.3. Biochemical composition of NRFP

The total carbohydrate was estimated using the phenol-sulfuric acid method using glucose as standard [26]. The protein content was determined using the Bradford assay with bovine serum albumin as standard [27]. Total neutral sugar, total phenolic compounds and uronic acid contents were obtained using respectively the sulfuric-resorcinol [28], Folin-Ciocalteu [29] and *m*-hydroxydiphenyl methods [30]. Carbon, hydrogen and nitrogen contents were carried out using elemental analyzer (Perkin Elmer analyzer, model 2400). Total starch and β-glucan assay kits (Megazyme) were used to determine both the presence of β-(1,3)/(1,4)-D-glucan and α-(1,4)/(1,6)-D-glucan and more particularly identify anomeric configuration of glucan structure.

2.4. Structural features of NRFP

2.4.1. Fourier-transform infrared spectroscopy (FT-IR) analysis

FT-IR spectra of NRFP were recorded on a VERTEX 70 FTIR instrument. The sample was dispersed on an ATR A225 diamante. Fifty scans were saved at room temperature (reference against air) with a spectrum range of 4000-400 cm^{-1}. The results were analyzed with OPUS 7.2 software.

2.4.2. High-pressure size exclusion chromatography analysis (HPSEC)

The average molecular weight of NRFP was evaluated by HPSEC (HPLC 1100 series, Agilent) with a differential refractive index (DRI) (RIDG1362, Agilent). Columns (TSKgel PWXK guard column, TSKgel PWXL 5000 and 3000, Tosoh Bioscience) were eluted with $NaNO_3$ 0.1M. Calibration was performed using pullulan standards (10 g/L) from 1.3 to 800 kDa. The sample was solubilized at 10 g/L in $NaNO_3$ 0.1M during 24 h under stirring before injection (20 µL). The number average molecular weight (M_n), weight average molecular weight (M_w) and polydispersity index (PDI) were determined using the following Equations 1-3:

$$M_n = \frac{\sum N_i M_i}{\sum N_i} \quad (1)$$

$$M_w = \frac{\sum N_i {M_i}^2}{\sum N_i M_i} \quad (2)$$

$$PDI = \frac{M_w}{M_n} \quad (3)$$

where N_i is the number of moles of polymer species and M_i the molecular weight of polymer species.

2.4.3. Monosaccharide composition

Trimethylsilyl-*O*-glycosides were prepared prior to GC/MS-EI analysis. NRFP (10 mg) was dissolved in TFA 2 M (1 mL) and heated at 120 °C for 90 min. The mixture was then evaporated under nitrogen stream. The derivatization of hydrolysates was possible using BSTFA: TMCS

(99:1) as described by Pierre et al. [31]. The trimethylsilyl-*O*-glycosides were finally solubilized into dichloromethane. The same procedure was repeated using standard monosaccharides (Ara, Fuc, Rha, Glc, Gal, Xyl, GlcA, Man and GalA) and subjected to GC/MS-EI analysis using an Agilent 6890 Series GC System coupled to an Agilent 5973 Network Mass Selective Detector, equipped with OPTIMA-1MS column (Macherey-Nagel; 30 m, 0.32 mm, 0.25 µm) [32]. The analytical conditions were the following ones, *i.e.* target ion: 40-800 m/z, injector line temperature: 250°C, trap temperature: 150°C, split ratio: 50: 1, helium pressure: 8.8 psi; helium flow rate: 2.3 mL/min, ionization: 70eV by electronic impact. The rise in temperature was programmed for a first step at 100°C during 3 min, an increment of 8°C/min up to 200°C for 1 min and then a final increment of 5°C/min up to 215°C.

2.4.4. Analysis of glycosyl-linkage composition

Pellets of solid NaOH/DMSO were prepared following the method of Ciucanu and Kerek [33] and used for the methylation step, which was adapted from Peña et al. [34]. The conversion of methylated residues to partially-O-methylated alditols acetate (PMAA) derivatives was adapted from the protocols of Blakeney et al. [35], Carpita and Shea [36] and Peña et al. (2012) [34]. PMAA derivatives were finally re-suspended into 200 µL of dichloromethane. Analyses were carried out by GC/MS-EI using the same apparatus as previously described. The rise in temperature was programmed for a first step at 80°C during 2 min, an increment of 30°C/min up to 170°C then a second increment of 4°C/min up to 240°C and a final level at 240°C for 20 min. Note that the samples were injected in splitless mode.

2.4.5. X-ray diffraction (XRD) analyses

The XRD pattern of NRFP was recorded at room temperature by a Siemens Bruker D5000 X-ray diffractometer (Siemens, Texas, USA). The samples were collected in the 2θ range 5° to 60° with a step size of 0.02° and a counting time of 0.78 s/step.

2.5. Biological properties of NFRP

2.5.1. Antioxidant activities *in vitro*

2.5.1.1 Total antioxidant capacity

This test was carried using the method described by Prieto et al. [37]. Different concentrations (2-12 mg/mL) of the sample were prepared. Then, 1 mL of the reagent solution of sulfuric acid, sodium phosphate and ammonium molybdate at concentrations of 0.6 M, 28 mM and 4 mM, respectively, were mixed with 0.1 mL of various concentrations. The tubes were incubated in a boiling water bath at 95°C for 90 min. After cooling the absorbance was measured at 695 nm. Vitamin C was used as positive control.

2.5.1.2. DPPH radical scavenging assay

The effect of NRFP on DPPH radical was determined following the method reported by Bounatirou et al. [38] with slight modifications. 500 µL of different concentrations (0.25-4 mg/mL) of NRFP were mixed with 125 µL DPPH methanolic solution (0.02% w/v) and 375 µL of methanol. The control tube was prepared using all reagents except the polysaccharide while ascorbic acid was used as the positive control. After 30 min of incubation in the dark, the absorbance was measured at 515 nm. NRFP scavenging activity on DPPH radical was calculated using Equation 4.

$$\text{Inhibition (\%)} = \frac{\text{Absorbance of control} - \text{Absorbance of sample}}{\text{Absorbance of control}} \times 100 \qquad (4)$$

2.5.1.3. Hydrogen peroxide (H_2O_2) scavenging assay

This test was done using the method of Liu et al. [39]. One milliliter of the sample with different concentration (0.1-5 mg/mL) was mixed with 2.4 mL of phosphate buffer (0.1 M, pH 7.4) and 0.6 mL of H_2O_2 solution (40 mM). The mixture was shaken vigorously and incubated at room temperature for 10 min. Ascorbic acid was used as positive control. The absorbance was measured at 230 nm. The scavenging activity was calculated using Equation 4.

2.5.1.4. Hemolysis inhibitory assay

This assay was conducted using H_2O_2 as an inducer of oxidative stress *in vitro*. EDTA tubes containing 15 mL of fresh blood were centrifuged for 15 min at 1,000 rpm to obtain red blood cells (RBCs). The latter were suspended in phosphate buffer solution (PBS) (10 mM, pH 7.4) and centrifuged at 4500 rpm at 4°C for 10 min. The erythrocytes were washed 3 times with PBS and finally diluted in PBS to give a solution at 2% (w/v). Serial dilutions of polysaccharide ranging from 10 to 250 µg/mL were prepared in PBS. 500 µL of H_2O_2 at 7.5 mM were used to induce hemolysis. After 1h of incubation at 37°C, the absorbance of the supernatant was measured at 540 nm. Ascorbic acid (5-200 µg/mL) was the positive control. Hemolysis inhibition (%) was calculated using Equation 5.

$$\text{Hemolysis inhibition}(\%) = \frac{1-\text{Absordance of sample}}{\text{Absorbance of control}} \times 100 \qquad (5)$$

2.5.2. Anti-hyperlipidemic activity *in vivo*

2.5.2.1. Experimental animals and toxicity study

The anti-hyperlipidemic effect of NRFP was tested on *Swiss albino* male mice of about 25-28 g body weight (BW). Animals were cared according to the Tunisian code of practice for the Care and Use of Animals for Scientific Purposes and the European convention for the protection of vertebrate animals used for experimental and other scientific purposes (Council of Europe No 123, Strasbourg, 1985). For the toxicity study, five groups (n = 6) were treated with different doses of NRFP (75, 125, 250, 500, and 1000 mg/kg of BW) and compared to the control group for the presence of toxic symptoms and death rate within 12 and 24 hours. Also, at the end of the study, the mice were sacrificed, and histopathological changes were denoted.

2.5.2.2. Induction of hyperlipidemia

Seven groups of mice, six in each received the following treatment:

Group-I: control group; mice received normal saline solution.

Group-II: NRFP treated control group; mice were orally (p.o.) treated with NRFP (500 mg/kg, b.w.) for 7 days

198 Group-III: Reference drug treated control group; mice were orally administered with atorvastatin
199 (10 mg/kg, b.w., p.o.) for 7 days [40].
200 Group-IV: Hyperlipidemia in mice was induced by a single intraperitoneal injection of Triton X-
201 100 (100 mg/kg, b.w., ip) in normal saline solution [41].
202 Group-V: Hyperlipidemic mice treated with low dose of NRFP (250 mg/kg, b.w., p.o.) for 7
203 days.
204 Group-VI: Hyperlipidemic mice treated with high dose of NRFP (500 mg/kg, b.w., p.o.) for 7
205 days.
206 Group-VII: Hyperlipidemic mice treated with atorvastatin (10 mg/kg, b.w., p.o.) for 7 days.
207 *2.5.2.3. Preparation of samples*
208 Twenty-four hours after the last treatment, animals were sacrificed by cervical decapitation
209 under light ether anesthesia. The serum was collected by centrifugation of the whole blood at
210 3500 rpm for 15 min at 4℃ and stored at -80 °C until analysis. Liver and heart samples were
211 quickly removed. One part was washed in ice-cold 1.15% potassium chloride solution,
212 homogenized into 2 ml ice-cold buffer (pH 7.4) and centrifuged for 30 min at 9000 rpm, 4 °C.
213 The collected supernatants were stored at -20 °C until the analysis. The other parts of tissues
214 were fixed immediately in 10% formalin for histopathological examination.
215 *2.5.2.4. Determination of lipid profile parameters*
216 Triglycerides (TG), total cholesterol (TC), high-density lipoprotein (HDL)-cholesterol, low-
217 density lipoprotein (LDL)-cholesterol were measured using an auto-analyzer (Roche Cobas C
218 311, Germany). Very low-density lipoprotein-cholesterol (VLDL-C), cardiac index (CI),
219 atherogenic index (AI) and coronary artery index (CAI) were calculated following Equations (6)-
220 (9) [42, 43].

221 $$VLDL - C = \frac{TG}{5} \qquad (6)$$

222 $$CI = \frac{TC}{HDLc} \qquad (7)$$

$$AI = \frac{(Total\ cholesterol - HDLc)}{HDLc} \quad (8)$$

$$CAI = \frac{LDLc}{HDLc} \quad (9)$$

2.5.2.5. Determination of lipid peroxidation levels

To estimate the degree of lipid peroxidation in liver and heart tissues, 100 µl of each homogenate supernatants were added to 100 µl of trichloroacetic acid (TCA, 5%) and the mixture were centrifuged at 3000 rpm for 10 min. After that, 100 µl of the supernatant and 200 µl of thiobarbituric acid reagent (TBA, 0.67% w/v) were incubated for 15 min on a boiling water bath. The level of lipids peroxidation was measured as thiobarbituric acid reactive substances (TBARS) and was calculated as malondialdehyde (MDA) formation, in accordance with the method of Draper and Hadley, [44] and expressed in nmoles/mg of protein.

2.5.2.6. Serum biochemical analysis

Serum liver biomarkers, *i.e.* alanine aminotransferase (ALT), aspartate aminotransferase (AST) and lactate dehydrogenase (LDH) were assayed using commercial reagent kits from Biomaghreb (Tunisia).

2.5.3. Histopathological observations

Liver and heart sections fixed in 10% formalin were washed with distilled water and treated by a series of alcohol baths and embedded in paraffin. Next, they were cut at 4-6 µm thickness, stained with hematoxylin-eosin and observed under a microscope. Meanwhile, 10 µm-frozen liver tissues were cut using a cryostat followed by quantitative analysis of lipid deposition by Oil red-O staining using Harris haematoxylin for nucleus coloration, as described by Han et al. (2015) [45]. Tissues preparations were observed and micro-photographed under a light Olympus CX31 microscope.

2.6. Statistical analysis

Statistical analysis was performed using the SPSS software program (PASW Statistics 18.0). All data were analyzed using one-way analysis of variance (ANOVA) and Student's t-test. Differences were considered significant at $p < 0.05$.

3. Results and discussion

3.1. NRFP composition

The results of chemical properties of NRFP are shown in Table 1. The extraction yield of NRFP was about 8.65% (w/w), which was lower than for a polysaccharide extracted from *N. tangutorum* fruits (14.01%) [46]. The carbohydrate content of NRFP measured by the phenol-sulfuric acid method was of 67.03% and that of protein 18.67%. High protein content was already reported for *Citrus aurantium* L. polysaccharides (17.01%) and chickpea flours water-soluble polysaccharides (11.22%) [47, 48]. However, Khemakhem et al. [49] reported lower protein content for *Olea europaea* L. polysaccharides (1.07%). Indeed, the deproteination and extraction procedures played a significant role in the protein content of polysaccharides. The phenolic compounds content was close to 5.46%. Enzymatic assays showed the absence of α-(1,4)/(1,6)-D-glucan from starch material (0.02%) inside NRFP. The elemental analysis of NRFP showed that carbon and hydrogen contents were 5.03% and 1.00% respectively. The ratio of carbon to hydrogen was consistent with the ratio of other polysaccharides [50].

The homogeneity and molecular weight of NRFP were evaluated using HPSEC system (Fig.1S). NRFPP showed a molecular weight around 66.5 x 10^3 g/mol with a low PDI value (1.18) highlighting the low polydispersity of NRFP (Table 2). The monosaccharide analysis (Fig. 2S) of NRFP after its acidic hydrolysis showed that it contained Glc, GalA, Ara and Rha. The predominant monosaccharides were Glc and GalA with a molar ratio of 41.4% and 30.5%, respectively. The minor constituents were Ara (11.8%) but mainly Rha with a molar ratio of 3.71%. These results were consistent with the colorimetric assays (Table 1). This composition was slightly different from the fruit polysaccharides isolated from *N. tangutorum* which was

mainly composed of Glc for NTWP-I and Rha, Gal, Glc, Ara and Man for NTWP-II after a separation on DEAE cellulose column [46]. All the above differences might be due to the species of plants, plant state, extraction, and purification methods [51]. It is important to point out that, up to now, the research on the purification, structural and biological characterization of polysaccharides of the genus *Nitraria* is very limited; on the contrary to other phytochemicals (for example alkaloids or flavonoids) [25,52].

3.2. FT-IR spectra

The FTIR spectrum of NRFP illustrated the typical characteristic signals of polysaccharides (Fig. 1A). The band at 3281 cm^{-1} showed strong hydroxyl groups signals of polysaccharides and water. The absorption bands at around 1607, 1231 and 1015 cm^{-1} belonged to the C−H vibration of the polysaccharide [53, 54]. The characteristic absorption at 1738 cm^{-1} was allocated to a rhamnogalacturonan structure in NRFP [55]. The absorbance band at 1607 cm^{-1} was attributed to carbonyl ester (C=O) groups [56], showing the presence of uronic acids in NRFP. This result was in agreement with the GC/MS-EI analysis that galacturonic acid was detected. The absorption band at 1403 cm^{-1} was attributed to C−O symmetric stretching vibration of the carboxyl group. The areas between 1200 - 800 cm^{-1} were a typical fingerprint for carbohydrates. These include C−O−C glycosidic bond vibrations and C−O−H links [57]. Moreover, the peak at 763 cm^{-1} might be attributed to the existence of β-configuration of pyranoses [58].

3.3. X-ray diffraction

The X-ray diffraction was used to examine the amorphous or crystalline structure of NRFP (Fig. 1B). The diffraction curve of NRFP showed a series of sharp peaks at 15°, 27.51°, 32.12°, 40.91°, 46.58° and 56.54° (2θ) suggesting a large degree of crystallinity. Combined to a broad peak at 21.57° (2θ), these results highlighted a crystalline backbone inside the amorphous structure of NRFP, which was consistent with other polysaccharides [50].

3.4. Glycosyl-linkage analysis

The PMAA derived from NRFP were subjected to GC/MS-EI analysis with the aim to identify the glycosidic linkages (Table 3, Figure 3S). The results revealed the exclusive presence of main residues of 1,3-linked Glc*p* (26.30%), 1,4-linked Gal*p* (28.7%), 1,3,6-linked Glc*p* (10.2%), terminal Gal*p* (9.33%), terminal Glc*p* (8.72%) as well as units of Ara*f* (9.41%) and Rha*p* (4.48%). This composition agreed with that obtained after TMS derivatization (Table 2) since the fraction was essentially composed of glucose (45.2%), galactose and galacturonic acid (38.0%), arabinose (12.3%) as well as rhamnose (4.48%) residues. These results suggested that NRFP was a glucan composed of (1→3)-linked D-Glc*p* as main backbone co-extracted with a pectin structure, and probably some HGA (Homogalacturonan) and RG-1 (RhamnoGalacturonan I) segments according to the following pattern presented in Fig. 2. This result was surprising regarding the low dispersity found in the fraction. The *β*-configuration was confirmed regarding the absence of starch material using a total starch assay kit (Table 1), which was consistent with the results obtained by Ni et al. [59], the observation made by FTIR and the partial hydrolysis using a beta glucan assay specific to *β*-(1,3)/(1,4)-glucan (data not shown). The presence of 1,3,6-linked Glc*p* residues (10.2%) showed that the glucan main backbone of NRFP could be a →3)-*β*-D-Glc*p*-(1→ glucan branched in *O*-6 positions. The ratio of total terminal residues (8.72%) was closed to the branched residues (10.2%), confirming again the good attribution and quantification of ramifications along the polysaccharide main chains. The pectin structure in NRFP fraction was probably a homogalacturonan (HGA) composed of →4)-*β*-D-Gal*p*A-(1→ as main chain with the presence of few 1,2-linked-Rha*p* and 1,2,4)-linked-Rha*p* involved in RG1 structure. The presence of terminal *β*-D-Gal*p*, 1,5-linked *α*-L-Ara*f*, 1,2,5-linked *α*-L-Ara*f* and 1,3,5-linked *α*-L-Ara*f* residues as well as 1,4-linked Galp could correspond to galactan, arabinane or arabinogalactane side chains. These conclusions were in accordance with the work of Ni et al. [59] which showed the presence of glucan and RG1 structures in a fraction obtained from *Nitraria tangutorum* Bobr. Fruits.

3.5. *In vitro* antioxidant activities

The antioxidant activities of NRFP were investigated using three complementary assays, namely the phosphomolybdenum test, the scavenging ability of hydrogen peroxide and DPPH (Fig. 3). The overall antioxidant activity of NRFP at different concentrations, measured by the phosphomolybdenum assay, is shown in Fig. 3A. The results revealed that the antioxidant activity of NRFP increased along with increasing concentrations from 2 to 12 mg/mL. The maximum of 80.89% inhibition was detected at the concentration of 12 mg/mL. At this concentration, vitamin C, used as positive control, showed an antioxidant activity of 93.36%. The half maximal inhibitory concentration (IC_{50}) value of the polysaccharide was determined to be close to 7.82 mg/mL, whereas, vitamin C showed an IC_{50} value of 2.03 mg/mL. Moreover, the DPPH radical scavenging activities of NRFP and vitamin C are shown in Fig. 3B. The scavenging rates of NRFP were found in the range of 25.28%-77.72% from 0.25-4 mg/mL. The IC_{50} values were estimated at 870 and 380 µg/mL for NRFP and vitamin C, respectively. The results revealed that the scavenging ability of NRFP was higher when compared to that of polysaccharides extracted from *N. tangutorum* fruits [46]. It has been considered that the antioxidant activities of polysaccharides are influenced by their structure and chemical composition. Our research indicated that NRFP contained high uronic acids and protein contents, which have been reported to be effective in better antioxidant activity management [60]. Furthermore, we assumed that the strong antioxidant activity of NRFP may be related to the presence of functional groups, such as C=O and OH [61]. Likewise, it is possible that the monosaccharide composition of NRFP including Rha, Glc, GalA, and Ara might explain its potent radical scavenging activity [62].

The *in vitro* hydrogen peroxide scavenging activity of NRFP was also tested. As illustrated in Fig. 3C, all concentrations showed a concentration-dependent scavenging activity towards H_2O_2. At 5 mg/mL, the H_2O_2 scavenging activity of NRFP was closed to 79.25%. These results were consistent with other reports involving natural polysaccharides including pectin HG/RG1 fractions [63]. Moreover, this antiradical activity was in accordance with that depicted in the

DPPH radical scavenging activity, indicating that NRFP possessed a certain antioxidant effect. Besides the chemical and monosaccharide composition, an electron-transfer mechanism also might affect the bioactivity of NRFP [7, 51]. Thus, NRFP could be considered as potential ROS scavenger not only through a single factor but a combination of diverse factors. However, due to the unavailability of complete structural characterization of NRFP, these effects and underlying mechanisms still incomplete, and future studies will be needed.

3.6. Inhibition of erythrocyte oxidative hemolysis induced by H_2O_2

Numerous *in vitro* and *in vivo* investigations have demonstrated that reactive oxygen species (ROS) produced by endogenous and exogenous sources affect many parameters of erythrocyte function, which increases oxidative stress [64, 65]. The later can cause disruption of the erythrocyte membranes and even induce hemolysis, resulting in the liberation of hemoglobin into plasma. Among the different ROS, the hydrogen peroxide is widely considered as a cytotoxic agent, because it induces a threat to the integrity of the erythrocytes and causes various biochemical perturbations [66]. In this study, H_2O_2-induced oxidative stress damage in erythrocytes was used to assess the antioxidant activity of NRFP. As seen in Fig. 3D, the hemolysis induced by H_2O_2 was significantly inhibited with the increment in NFRP concentrations, which was consistent with the results of the aforementioned antioxidant activities. At the concentration of 250 μg/mL, the inhibitory rate of hemolysis was 84.69 %. The IC_{50} value of NRFP on H_2O_2-induced hemolysis was 66.2 μg/mL. This significant hemolysis inhibitory activity was much less effective than that of vitamin C (IC_{50}= 18.91 μg/mL) but higher than those reported for polysaccharides isolated from *Diaphragma juglandis* [67]. Despite the limited data available on the protective effect of polysaccharide on oxidative stress-induced human erythrocytes injuries, it could be possible that the anti-hemolytic activity of NRFP occurs mainly due to their active hydroxyl groups that can scavenge ROS (like H_2O_2) [68].

3.7. Anti-hyperlipidemic activity *in vivo*

3.7.1. Toxicity study

The estimation of the acute oral toxicity of the polysaccharide attested that it was nontoxic and did not generate any behavioral changes with the doses of 75-1000 mg/kg during the 24h of the observation period. Moreover, the light microscopic examination of all vital organs such as the heart, kidneys, and liver tissues revealed normal histological structures (data not shown).

3.7.2. Effects of NRFP on serum lipid profiles and lipoproteins

In this study, dyslipidemia has been successfully induced in mice using Triton X-100. This non-ionic detergent has been chosen due to its availability and appropriateness. Clinically, the alterations in lipid profile were principally investigated by measuring the levels of TG, TC, LDL-C, VLDL-C and HDL-C. Elevated TG levels accelerated risks for coronary heart diseases and, therefore, the decrease in TG levels using natural polysaccharides from edible and medicinal plants will be advantageous to prevent from heart attacks and the development of atherosclerosis.

Following Triton X-100 injection, serum TC, TG levels, and LDL-C were significantly raised by 68.18%, 72.47%, and 41.48%, respectively, while HDL-C was significantly reduced by 36.48% in the hyperlipidemic control group compared with the normal control mice, demonstrating that hyperlipidemia was readily induced (Fig. 4A-E) [41]. Oral treatment with NRFP (250-500 mg/kg) and atorvastatin (10 mg/kg) for seven days after Triton X-100 injection showed that the TC, TG and LDL levels remarkably decreased and the levels of HDL-C were increased by 27.19%, 54.38% and 51.75% in the groups treated with 250 and 500 mg/kg of NRFP and 10 mg/kg of atorvastatin respectively, in comparison to the hyperlipidemic control group ($p < 0.01$). These results suggested that NRFP had a hypolipidemic effect against Triton X-100-induced hyperlipidemia and liver injury. Similar dyslipidemic profiles have been highlighted for natural polysaccharides from plants and multiple mechanisms have been suggested for the restoration of

400 the lipid profiles. For example, Yang et al. [9] found that polysaccharide from *Cyclocarya*
401 *paliurus* can ameliorate hyperlipidaemia by modulating the fatty acid synthesis genes expression
402 like fatty acid synthase and acetyl-CoA carboxylase. According to Hu et al. [69] the possible
403 mechanism of antihyperlipidemic effect of polysaccharides may be associated with the
404 modulation of the activities of lipid metabolism-related enzymes including Peroxisome
405 Proliferator-activated Receptor (PPARγ and PPARδ). In addition, Ren et al. [70] showed that
406 polysaccharide from *Enteromorpha prolifera* could enhance lipid profiles by suppressing the
407 expression of sterol regulatory element binding protein.
408 3.7.3. Atherosclerotic and cardioprotective indices
409 Hyperlipidaemia is a major factor in the development of cardiovascular and coronary diseases.
410 Accordingly, it is important to calculate atherosclerotic indexes and cardioprotective indices of
411 NRFP. The increased in the indices of AI, CAI and CI in Triton X-100 induced hyperlipidemic
412 mice have been already reported [40,71].
413 Compared with the hyperlipidemic control group after orally administered for seven days, the
414 CAI, CI and AI indices of the group treated with 500 mg/kg of NRFP were significantly
415 decreased by 39.51%, 41.74%, and 59.63%, respectively (Fig. 4F-G-H). Atorvastatin-treated
416 mice also revealed a decline in CAI (by 39.97%), CI (by 43.09%) and AI (by 61.56%) compared
417 to the hyperlipidemic control mice. The results suggested that NRFP might be used as a main
418 alternative hypolipidemic agent, as well as to prevent or reduce cardiovascular and coronary
419 diseases.
420 *3.7.4. Effects of NRFP on lipid peroxidation levels*
421 Based on the examination of oxidative stress biomarkers, there was a considerable increase in
422 MDA levels both in the liver and heart tissues in the mice treated with Triton X-100-induced
423 hyperlipidemia, when compared to the control group, suggesting that a severe oxidative stress
424 had been occurred in the heart and liver (Fig. 5D). These results were in agreement with other
425 papers revealing that the treatment of animals with Triton X-100 promotes the production of free

radicals and ROS, leading to oxidative stress [41]. However, this increase tended to be alleviated by dietary supplementation of NRFP, in fact, the treatment of animals with NRFP had notably lower MDA levels compared to the Triton X-100 treated group. Briefly, for the mice treated with NRFP at the two dosages of 250 and 500 mg/kg, the hepatic MDA levels were significantly decreased by 36.34% and 55.25% respectively, compared to that of the hyperlipidemic group (Fig. 5). After the treatment with NRFP at the dose of 250 and 500 mg/kg, the cardiac MDA contents decreased significantly by 17.43% and 45.10% respectively, compared with those of the hyperlipidemic mice. Similarly, when tested at a dose of 10 mg/kg atorvastatin as a positive control also effectively prevent the lipid peroxidation in heart and liver tissues. A comparable decline in the level of MDA following administration of polysaccharides from *Termitomyces albuminosus* [12] and *Cyclocarya paliurus* [9] to hypercholesterolemic mice has previously been highlighted.

3.7.5. Effects of NRFP on serum hepatic marker enzymes

The hepatic damages could also be investigated measuring the serum antioxidant activities of AST, ALT, and LDH. As illustrated in Fig. 5, significant increases in the serum activities of ALT, AST, and LDH were observed in Triton-X 100-induced hyperlipidemia in mice as compared to the control group, respectively, suggesting that serious oxidative injuries had happened in the liver. The toxic effects of Triton-X 100 on the liver were related to the disruption of hepatocyte membrane permeability and consequently leading to the liberation of these enzymes into the blood circulation [12]. However, the treatment of Triton X-100-induced hypercholesterolemic mice with NRFP significantly reduced these serum enzyme levels. As shown in Fig. 5, the serum activities of AST, ALT, and LDH in the hyperlipidemic mice treated with NRFP at the dose of 500 mg/kg reduced markedly by 25.20%, 21.34% and 33.50%, respectively in comparison with the hyperlipidemic group. These results suggested that NRFP maintained membrane integrity and limited the escape of hepatic enzymes. Besides, when tested at a dosage of 10 mg/kg, atorvastatin-treated mice also indicated a remarkable decline of the

ALT, AST, and LDH enzyme activities in Triton X-100-induced oxidative damage compared to that of the hyperlipidemic treated group. All the above results suggested that the NRFP supplementation is effective for protection against hyperlipidemia and hepato-cardiac damages in Triton X100-treated animals.

3.7.6. Histopathological evaluation of liver and heart

In the current study, the hypolipidemic effects of NRFP were confirmed by the histological examination of liver and heart tissues.

The liver section in the control group, group treated with NRFP (500 mg/kg, b.w.) and atorvastatin (10 mg/kg, bw., p.o.) (Fig. 6I) showed normal hepatocytes morphology and the absence of histopathological alteration. However, the mice treated with Triton-X 100 (100 mg/kg, bw) revealed serious loss of liver histoarchitecture, congestion in the central vein, hepatic necrosis, inflammatory cell infiltration, fat vacuoles and obliterated sinusoids. The hyperlipidemic mice treated with NRFP at 250 mg/kg, showed an improved liver architecture, although the congestion in the central vein and inflammatory cell infiltration still persists. The liver of hyperlipidemic mice fed with NRFP at a dose of 500 mg/kg and atorvastatin, respectively, revealed normal histology of the liver tissue with intact central vein and well-preserved cytoplasm comparable to the control group.

Cardiac tissues in the groups treated with normal saline, NRFP at 500 mg/kg, b.w. and atorvastatin (Fig. 6II) showed the absence of histopathological alteration with regularly arranged myocardial fibers. However, heart sections of animals treated with Triton X-100 revealed degeneration of myocardial cell, cytoplasmic vacuolization, and cardiac hypertrophy. The hyperlipidemic mice administered with NRFP at 500 mg/kg, b.w. was more effective in cardiac protection than was the dose of 250 mg/kg, b.w. Interestingly, the myocardium of hyperlipidemic mice treated with NRFP (250 mg/kg) showed improved heart architecture, although the

478 separation of cardiac myofibers still persists. The myocardial cell in sections of heart taken from
479 the high-dose of NRFP-treated group revealed a normal appearance, with a well-preserved
480 cytoplasm. A similar pattern of cardiac histoarchitecture was observed in mice from groups
481 treated with atorvastatin compared to that of control groups. Our experimental results support
482 those of others reports who showed that polysaccharides administration improved the
483 histopathological alteration in hyperlipidemic mice [9,12,70].
484 To further justify the hypolipidemic effect of NRFP, cold liver portions were colored by oil Red
485 O to observe the accumulation of lipid droplets (Fig. 6III). The liver sections in the control,
486 NRFP, and atorvastatin-treated mice revealed that the lipid droplets were absent. However,
487 multiple lipid droplets were recorded in the liver of the hyperlipidemic mice. Meanwhile, the
488 liver section of the hyperlipidemic mice treated with NRFP showed a remarkable reduction in
489 lipid droplets corroborating the ability of NRFP to prevent the accumulation of fats in the liver.
490 These results were consistent with previous reports [72].
491 **Conclusion**
492 In this study, an enriched polysaccharide fraction called NRFP was obtained by hot water
493 extraction. The molecular weight of the polysaccharidic fraction was about 66.5 kDa. NRFP was
494 composed of glucose, arabinose, galacturonic acid, galactose, and rhamnose with a molar ratio of
495 41.4%, 11.8%, 30.5%, 12.6% and 3.7% respectively. The structural investigations highlighted
496 the presence of a β-(1,3)-glucan branched in *O*-6 position. The presence of a HGA-RG1 structure
497 in NRFP was not negligible and was already observed in the literature for other species of
498 *Nitraria*. Further work should be needed to identify if the HGA-RG1 is associated to the glucan
499 structure inside the fruits. Beside, i*n vitro,* the results advised that the NRFP exhibited
500 appreciable antioxidant potentials against DPPH and hydrogen peroxide in dose-dependent
501 manners. Meanwhile, NRFP exhibited high hepatoprotective and hypolipidemic effects *in vivo*.
502 Based on these findings, we suggested that NRFP may be selected as a potential antioxidant and

anti-hyperlipidemic agents for the treatment of cardiovascular disease and other hyperlipidemia complications.

Acknowledgments

The present study was supported by the Tunisian Ministry of Higher Education and Scientific Research, Tunisia.

References

[1] H.F. Tan, C.Y. Gan, Polysaccharide with antioxidant, α-amylase inhibitory and ACE inhibitory activities from *Momordica charantia*, Int. J. Biol. Macromol. 85 (2016) 487-496.

[2] I.S. Silva, L.A. Nicolau, F.B. Sousa, S. de Araújo, A.P. Oliveira, T.S. Araújo, L.K.M. Souza, C.S Martins, P.E.A. Aquino, L.L. Carvalho, R.O. Silva, P.J. Rolim-Neto, Medeiros, Evaluation of anti-inflammatory potential of aqueous extract and polysaccharide fraction of *Thuja occidentalis* Linn. in mice, Int. J. Biol. Macromol. 105 (2017) 1105-1116.

[3] Y.J. Liu, J.L. Du, L.P. Cao, R. Jia, Y.J. Shen, C.Y. Zhao, P. Xu, G.J. Yin, Anti-inflammatory and hepatoprotective effects of *Ganoderma lucidum* polysaccharides on carbon tetrachloride-induced hepatocyte damage in common carp (*Cyprinus carpio* L.) Inter, Immunopharmacol. 25 (2015) 112-120.

[4] I.C. Ferreira, S.A. Heleno, F.S. Reis, D. Stojkovic, M.J.R. Queiroz, M.H. Vasconcelos, M. M. Sokovic, Chemical features of Ganoderma polysaccharides with antioxidant, antitumor and antimicrobial activities, Phytochem. 114 (2015) 38-55.

[5] S. Li, A. Gao, S. Dong, Y. Chen, S. Sun, Z. Lei, Z. Zhang, Purification, antitumor and immunomodulatory activity of polysaccharides from soybean residue fermented with *Morchella esculenta*, Int. J. Biol. Macromol. 96 (2017) 26-34.

[6] J. Wang, S. Hu, S. Nie, Q. Yu, M. Xie, Reviews on mechanisms of *in vitro* antioxidant activity of polysaccharides, Oxid. Med. Cell. 2016 (2016).

[7] Z. Mzoughi, vAbdelhamid, C. Rihouey, D. Le Cerf, A. Bouraoui, H. Majdoub, Optimized extraction of pectin-like polysaccharide from *Suaeda fruticosa* leaves: Characterization, antioxidant, anti-inflammatory and analgesic activities, Carbohydr. Polym. 185 (2018) 127-137.

[8] J.J. Haddad, Cytokines and related receptor-mediated signaling pathways, Biochem. Biophys. Res. Commun. 297 (2002) 700-713.

[9] Z. Yang, J. Wang, J. Li, L. Xiong, H. Chen, X. Liu, N. Wang, K. Ouyang, W. Wang, Antihyperlipidemic and hepatoprotective activities of polysaccharide fraction from *Cyclocarya paliurus* in high-fat emulsion-induced hyperlipidaemic mice, Carbohydr. Polym. 183 (2018) 11-20.

[10] N. Xu, Z. Ren, J. Zhang, X. Song, Z. Gao, H. Jing, S. Li, S. Wang, L. Jia, Antioxidant and anti-hyperlipidemic effects of mycelia zinc polysaccharides by *Pleurotus eryngii* var. tuoliensis, Int. J. Biol. Macromol. 95 (2017) 204-214.

[11] C.P. Cannon, Cardiovascular disease and modifiable cardiometabolic risk factors, Clin. Cornerstone. 9 (2008) 24-41.

[12] H. Zhao, S. Li, J. Zhang, G. Che, M. Zhou, M. Liu, C. Zhang, N. Xu, L. Lin, Y. Liu, L. Jia, The antihyperlipidemic activities of enzymatic and acidic intracellular polysaccharides by *Termitomyces albuminosus*, Carbohydr. Polym. 151 (2016) 1227-1234.

[13] S. Lim, P.C. Oh, I. Sakuma, K.K. Koh, How to balance cardiorenometabolic benefits and risks of statins, Atherosclerosis. 235 (2014) 644–648.

549 [14] F. Senejoux, C. Girard, H.A. Aisa, M. Bakri, P. Kerram, A. Berthelot, F. Bévalot, C.
550 Demougeot, Vasorelaxant and hypotensive effects of a hydroalcoholic extract from the fruits
551 of *Nitraria sibirica* Pall. (Nitrariaceae), J. Ethnopharmacol. 141 (2012) 629-634.

552 [15] J.A. Duan, I.D. Williams, C.T. Che, R.H. Zhou, S.X. Zhao, Tangutorine: A novel β-
553 carboline alkaloid from *Nitraria tangutorum*, Tetrahedron. Letters. 40 (1999) 2593-2596.

554 [16] M.S. Rad, J.S. Rad, G.A. Heshmati, A. Miri, D.J. Sen, Biological synthesis of gold and
555 silver nanoparticles by *Nitraria schoberi* fruits, Open J. Adv. Drug. Delivery. 1 (2013) 174-
556 179.

557 [17] T. Ma, N. Hu, C. Ding, Q. Zhang, W. Li, Y. Suo, H. Wang, B. Bai, C. Ding, In vitro and in
558 vivo biological activities of anthocyanins from *Nitraria tangutorun* Bobr. Fruits, Food Chem.
559 194 (2016) 296-303.

560 [18] E. le Floc'h, Contribution a une étude Ethnobotanique de la Flore tunisienne, Ministere de
561 l'enseignement Superieure et de la Recherche Scientifique, (1952).

562 [19] J.H. Salem, I. Chevalot, C. Harscoat-Schiavo, C. Paris, M. Fick, C. Humeau, Biological
563 activities of flavonoids from *Nitraria retusa* (Forssk.) Asch. and their acylated derivatives,
564 Food Chem. 124 (2011) 486-494.

565 [20] M. Chaâbane, S. Maktouf, N. Sayari, S. Zouari, N. Zeghal, R. Ellouze Ghorbel, Antioxidant
566 and antimicrobial properties of the extracts from *Nitraria retusa* fruits and their applications
567 to meat product preservation, Ind. Crop. Prod. 55 (2014) 295-303.

568 [21] F. Zar Kalai, J. Han, R. Ksouri, A. El Omri, C. Abdelly, H. Isoda, Antiobesity effects of an
569 edible halophyte *Nitraria retusa* Forssk in 3T3-L1 preadipocyte differentiation and in
570 C57B6J/L mice fed a high fat diet-induced obesity, J. Evidence-Based Complementary
571 Altern. Med. 2013 (2013) 368658.

572 [22] M. Chaâbane, M. Koubaa, N. Soudani, A. Elwej, M. Grati, K. Jamoussi, T. Boudawara , S.
573 Ellouze Chaabouni, N. Zeghal, *Nitraria retusa* fruit prevents penconazole-induced kidney
574 injury in adult rats through modulation of oxidative stress and histopathological changes,
575 Pharma. Biol. 55 (2017) 1061-1073.

576 [23] M. Chaâbane, N. Soudani, K. Benjeddou, M. Turki, F. Ayadi Makni, T. Boudawara, N.
577 Zeghal, R. Ellouze Ghorbel, The protective potential of *Nitraria retusa* on penconazole-
578 induced hepatic injury in adult rats, Toxicol. Environ. Chem. 97 (2015) 1253-1264.

579 [24] A.A. Mohamed, S.I. Ali, F.K. El-Baz, S.R. Hussein, Comparative study of antioxidant
580 activities of *Nitraria retusa* and quantification of its bioactive components by GC/MS, Int. J.
581 Pharm. Sci. Rev. Res. 29 (2014) 241-246.

582 [25] T.S. Tulyaganov, F.K. Allaberdiev, Alkaloids from plants of the *Nitraria* genus. Structure
583 of sibiridine, Chem. Nat. Compd. 39 (2003) 292-293.

584 [26] M. Dubois, K.A. Gilles, J.K. Hamilton, P.T. Rebers, F. Smith, Colorimetric method for
585 determination of sugars and related substances, Anal. Chem. 28 (1956) 350–356.

586 [27] M.M. Bradford, A rapid and sensitive method for the quantitation of microgram quantities
587 of protein utilizing the principle of protein-dye binding. Anal. Biochem. 72 (1976) 248–254.

588 [28] M. Monsigny, C. Petit, A.C. Roche, Colorimetric determination of neutral sugars by a
589 resorcinol sulphuric acid micromethod, Anal. Biochem. 175 (1988) 525–530.

590 [29] V.L. Singleton, R. Orthofer, R.M. Lamuela-Raventós, Analysis of total phenols and other
591 oxidation substrates and antioxidants by means of folin-ciocalteu reagent, Methods Enzymol.
592 299 (1999) 152-178.

593 [30] N. Blumenkrantz, G. Asboe-Hansen, New method for quantitative determination of uronic
594 acids, Anal. Biochem. 54 (1973) 484–489.

595 [31] G. Pierre, J.M. Zhao, F. Orvain, C. Dupuy, G.L. Klein, M. Graber, T. Maugard, Seasonal
596 dynamics of extracellular polymeric substances (EPS) in surface sediments of a diatom-
597 dominated intertidal mudflat (Marennes-Oléron, France), J. Sea Res. 92 (2014) 26-35.

598 [32] F. Hentati, C. Delattre, A.V. Ursu, J. Desbrières, D.Le Cerf, C. Gardarin, S. Abdelkafi, P.
599 Michaud, G. Pierre, Structural characterization and antioxidant activity of water-soluble
600 polysaccharides from the Tunisian brown seaweed *Cystoseira compressa*, Carbohydr. Polym.
601 198 (2018) 589-600.

602 [33] I. Ciucanu, F. Kerek, A simple and rapid method for the permethylation of carbohydrates,
603 Carbohydr. Res. 131 (1984) 209-217.

604 [34] M.J. Peña, S.T. Tuomivaara, B.R. Urbanowicz, M.A. O'Neill, W.S. York, Methods for
605 structural characterization of the products of cellulose- and xyloglucan hydrolyzing enzymes,
606 Methods. Enzymol. 510 (2012) 121-139.

607 [35] A.B. Blakeney, P.J. Harris, R.J. Henry, B.A. Stone, A simple and rapid preparation of
608 alditols acetates for monosaccharide analysis, Carbohydr. Res. 113 (1983) 291–299.

609 [36] N.C. Carpita, E.M. Shea, Linkage structure of carbohydrates by gas chromatography-mass
610 spectrometry (GC-MS) of partially methylated alditol acetates, Analysis of Carbohydrates by
611 GLC and MS. (1989) 157-216.

612 [37] P. Prieto, M. Pineda, M. Aguilar, Spectrophotometric quantitation of antioxidant capacity
613 through the formation of a phosphomolybdenum complex: specific application to the
614 determination of vitamin E, Anal. Biochem. 269 (1999) 337-341.

615 [38] S. Bounatirou, S. Smiti, M.G. Miguel, L. Faleiro, M.N. Rejeb, M. Neffati, M.M. Costa,
616 A.C. Figueire do, L.G. Pedro, Chemical composition, antioxidant and antibacterial activities
617 of the essential oils isolated from Tunisian *Thymus capitatus* Hoff. et Link, Food Chem. 105
618 (2007) 146-155.

[39] J. Liu, J. Luo, H. Ye, Y. Sun, Z. Lu, X. Zeng, In vitro and in vivo antioxidant activity of exopolysaccharides from endophytic bacterium *Paenibacillus polymyxa* EJS-3, Carbohydr. Polym. 82 (2010) 1278-1283.

[40] N.M. Shafik, A. Baalash, A.M. Ebeid, Synergistic cardioprotective effects of combined chromium picolinate and atorvastatin treatment in triton X-100-induced hyperlipidemia in rats: impact on some biochemical markers. Biol. Trace. Element. Res. 180 (2017) 255-264.

[41] R. Gundamaraju, K.K. Hwi, R.K. Singla, R.C. Vemuri, S.B. Mulapalli, Antihyperlipidemic potential of *Albizia amara* (Roxb) Boiv. bark against Triton X-100 induced hyperlipidemic condition in rats, Pharmacogn. Res. 6 (2014) 267.

[42] M.J. Kang, E.K. Lee, S.S. Lee, Effects of two P/S ratios with same peroxidizability index value and antioxidants supplementation on serum lipid concentration and hepatic enzyme activities of rats, Clinica. Chimica. Acta. 350 (2004) 79-87.

[43] F. Kayamori, K. Igarashi, Effects of dietary nasunin on the serum cholesterol level in rats. Biosci. Biotechnol. Biochem. 58 (1994) 570-571.

[44] H.H. Draper, M. Hadley, Malondialdehyde determination as index of lipid peroxidation, Methods Enzymol. 186 (1990) 421-431.

[45] J.Y. Han, S. Lee, J.H. Yang, S. Kim, J. Sim, M.G. Kim, S.H. Ki, Korean Red Ginseng attenuates ethanol-induced steatosis and oxidative stress via AMPK/ Sirt1 activation, J. Ginseng. Res. 39 (2015) 105–115.

[46] B. Zhao, J. Liu, X. Chen, J. Zhang, J. Wang, Purification, structure and anti-oxidation of polysaccharides from the fruit of *Nitraria tangutorum* Bobr, RSC Advances. 8 (2018) 11731-11743.

641 [47] A.M. Ghribi, A. Sila, I.M. Gafsi, C. Blecker, S. Danthine, Attia, H. Bougatef, A. Besbes, S.
642 Structural, functional, and ACE inhibitory properties of water-soluble polysaccharides from
643 chickpea flours, Int. J. Biol. Macromol. 75 (2015) 276-282.

644 [48] Q.H. Wang, Z.P. Shu, B.Q. Xu, N. Xing, W.J. Jiao, B.Y. Yang, H.X. Kuang, Structural
645 characterization and antioxidant activities of polysaccharides from *Citrus aurantium* L, Int. J.
646 Biol. Macromol. 67 (2014) 112-123.

647 [49] I. Khemakhem, O. Abdelhedi, I. Trigui, M.A. Ayadi, M. Bouaziz, Structural, antioxidant
648 and antibacterial activities of polysaccharides extracted from olive leaves, Int. J. Biol.
649 Macromol. 106 (2018) 425-432.

650 [50] D. Suvakanta, M.P. Narsimha, D. Pulak, C. Joshabir, D. Biswajit, Optimization and
651 characterization of purified polysaccharide from *Musa sapientum* L. as a pharmaceutical
652 excipient, Food Chem. 149 (2014) 76-83.

653 [51] K. Zhu, Y. Zhang, S. Nie, F. Xu, S. He, D. Gong, G. Wu, L. Tan, Physicochemical
654 properties and in vitro antioxidant activities of polysaccharide from *Artocarpus heterophyllus*
655 Lam. Pulp, Carbohydr. Polym. 155 (2017) 354-361.

656 [52] Q. Du, H. Xin, C. Peng, Pharmacology and phytochemistry of the *Nitraria* genus, Mol.
657 Med. Reports. 11 (2015) 11-20.

658 [53] S. Palanisamy, M. Vinosha, M. Manikandakrishnan, R. Anjali, P. Rajasekar, T.
659 Marudhupandi, B. Vaseeharan, N.M. Prabhu, Investigation of antioxidant and anticancer
660 potential of fucoidan from *Sargassum polycystum*, Int. J. Biol. Macromol. 116 (2018) 151-
661 161.

662 [54] S. Palanisamy, M. Vinosha, T. Marudhupandi, P. Rajasekar, N.M. Prabhu, In vitro
663 antioxidant and antibacterial activity of sulfated polysaccharides isolated from *Spatoglossum*
664 *asperum*, Carbohyd. Polym. 170 (2017) 296-304.

665 [55] P.T. Kungel, V.G. Correa, R.C. Corrêa, R.A. Peralta, M. Soković, R.C. Calhelha, A. Bracht,
666 I.C.F.R. Ferreira, R.M. Peralta, Antioxidant and antimicrobial activities of a purified
667 polysaccharide from yerba mate (*Ilex paraguariensis*), Int. J. Biol. Macromol. 114 (2018)
668 1161-1167.

669 [56] Z. Liu, J. Dang, Q.Wang, M. Yu, L. Jiang, L. Mei, Y. Shao, Y. Tao, Optimization of
670 polysaccharides from *Lycium ruthenicum* fruit using RSM and its anti-oxidant activity, Int. J.
671 Biol. Macromol. 61 (2013) 127–134.

672 [57] H. Cheng, S. Feng, X. Jia, Q. Li, Y. Zhou, C. Ding, Structural characterization and
673 antioxidant activities of polysaccharides extracted from *Epimedium acuminatum*, Carbohydr.
674 Polym. 92 (2013) 63-68.

675 [58] J. Zhu, W. Liu, J. Yu, S. Zou, J. Wang, W. Yao, X. Gao, Characterization and
676 hypoglycemic effect of a polysaccharide extracted from the fruit of *Lycium barbarum* L,
677 Carbohydr. Polym. 98 (2013) 8-16.

678 [59] W. Ni, T. Gao, H. Wang, Y. Du, J. Li, C. Li, L. Wei, Bi. Hongtao, Anti-fatigue activity of
679 polysaccharides from the fruits of four Tibetan plateau indigenous medicinal plants, J.
680 Ethnopharmacol. 150 (2013) 529-535.

681 [60] H. Chen, M. Zhang, Z. Qu, B. Xie, Antioxidant activities of different fractions of
682 polysaccharide conjugates from green tea (*Camellia Sinensis*), Food Chem. 106 (2008) 559-
683 563.

684 [61] Z.B. Wang, J.J. Pei, H.L. Ma, P.F. Cai, J.K. Yan, Effect of extraction media on preliminary
685 characterizations and antioxidant activities of *Phellinus linteus* polysaccharides, Carbohydr.
686 Polym. 109 (2014) 49-55.

687 [62] D. Liu, J. Sheng, Z. Li, H. Qi, Y. Sun, Y. Duan, W. Zhang, Antioxidant activity of
688 polysaccharide fractions extracted from *Athyrium multidentatum* (Doll.) Ching, Int. J. Biol.
689 Macromol. 56 (2013) 1-5.

690 [63] J. Liu, S. Willför, C. Xu, A review of bioactive plant polysaccharides: Biological activities,
691 functionalization, and biomedical applications, Bioactive Carbohydr. Dietary. Fibre. 5 (2015)
692 31-61.

693 [64] B. Bukowska, B. Rychlik, A. Krokosz, J. Michałowicz, Phenoxyherbicides induce
694 production of free radicals in human erythrocytes: oxidation of dichlorodihydrofluorescine
695 and dihydrorhodamine 123 by 2, 4-D-Na and MCPA-Na, Food Chem. Toxicol. 46 (2008)
696 359-367.

697 [65] M. Miki, H. Tamai, M. Mino, Y. Yamamoto, E. Niki, Free-radical chain oxidation of rat red
698 blood cells by molecular oxygen and its inhibition by α-tocopherol, Arch. Biochem. Biophys.
699 258 (1987) 373-380.

700 [66] B. Tavazzi, D.D. Pierro, A.M. Amorini, G. Fazzina, M.T.B. Giardina, G. Lazzarino, Energy
701 metabolism and lipid peroxidation of human erythrocytes as a function of increased oxidative
702 stress, Eur. J. Biochem. 267 (2000) 684–689.

703 [67] Q. Meng, F. Chen, T. Xiao, L. Zhang, Inhibitory effects of polysaccharide from
704 *Diaphragma juglandis fructus* on α-amylase and α-d-glucosidase activity, streptozotocin-
705 induced hyperglycemia model, advanced glycation end-products formation, and H_2O_2-
706 induced oxidative damage, Int. J. Biol. Macromol. 124 (2019) 1080-1089.

707 [68] C.M. Zhang, S.H. Yu, L.S. Zhang, Z.Y. Zhao, L.L. Dong, Effects of several acetylated
708 chitooligosaccharides on antioxidation, antiglycation and NO generation in erythrocyte,
709 Bioorg. Med. Chem. Lett. 24 (2014) 4053-4057.

710 [69] W.B. Hu, J. Zhao, H. Chen, L. Xiong, W.J. Wang, Polysaccharides from *Cyclocarya*
711 *paliurus*: Chemical composition and lipid-lowering effect on rats challenged with high-fat
712 diet, J. Func. Food. 36 (2017) 262-273.

713 [70] Z. Ren, J. Li, N. Xu, J. Zhang, X. Song, X. Wang, Z. Gao, H. Jing, S. Li, C. Zhang, M. Liu,
714 H. Zhao, L. Jia, Anti-hyperlipidemic and antioxidant effects of alkali-extractable mycelia
715 polysaccharides by *Pleurotus eryngii* var. tuolensis, Carbohydr. Polym. 175 (2017) 282-292.

716 [71] N.S. Adigun, A.T. Oladiji, T.O. Ajiboye, Antioxidant and anti-hyperlipidemic activity of
717 hydroethanolic seed extract of *Aframomum melegueta* K. Schum in Triton X-100 induced
718 hyperlipidemic rats, South Afri. J. Botany. 105 (2016) 324-332.

719 [72] J.Y. Han, S. Lee, J.H. Yang, S. Kim, J. Sim, M.G. Kim, S.H. Ki, Korean Red Ginseng
720 attenuates ethanol-induced steatosis and oxidative stress via AMPK/ Sirt1 activation, J.
721 Ginseng. Res. 39 (2015) 105–115.

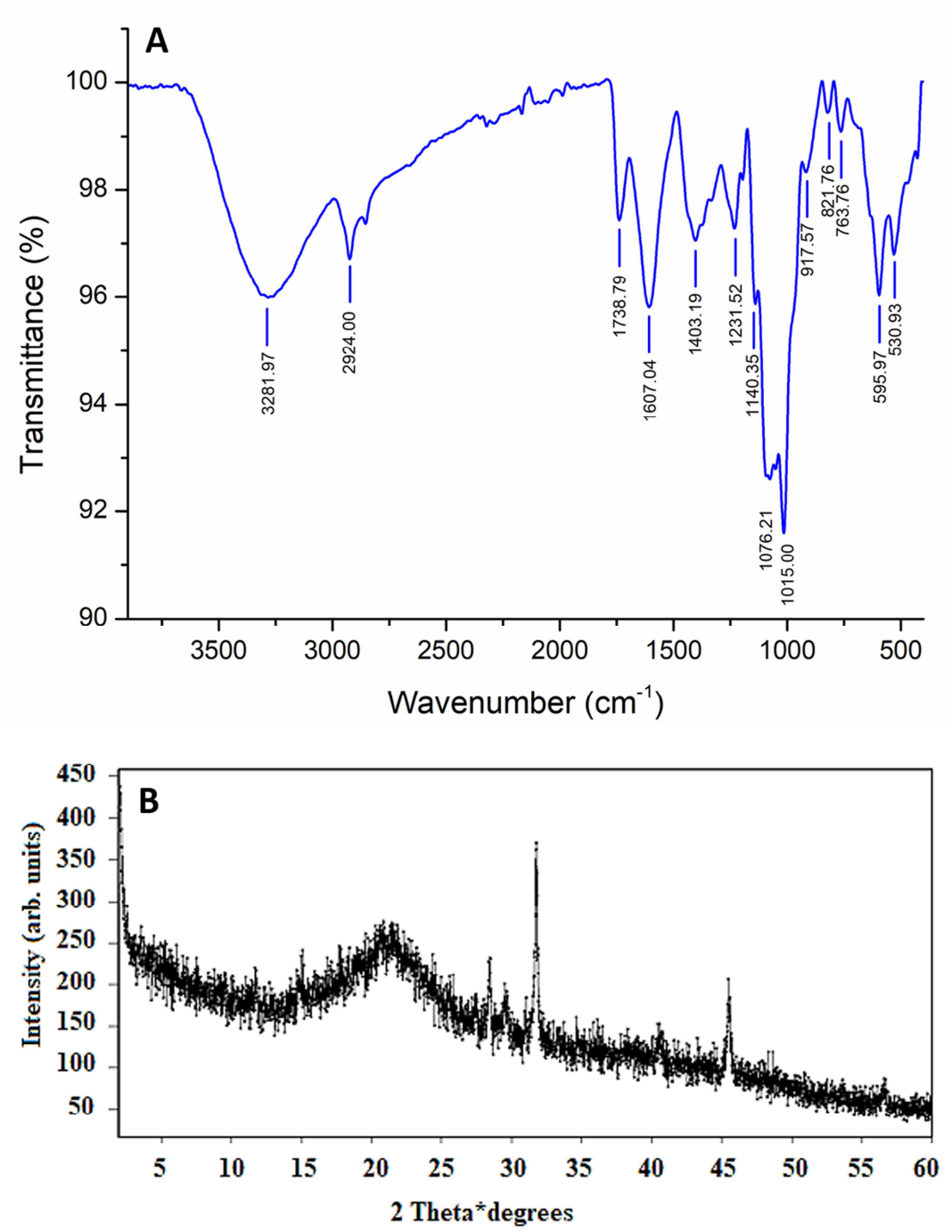

Fig. 1. (A) ATR-FTIR spectra of NRFP and **(B)** XRD profile of NRFP with scattering angles (2θ) ranging from 5 to 60°.

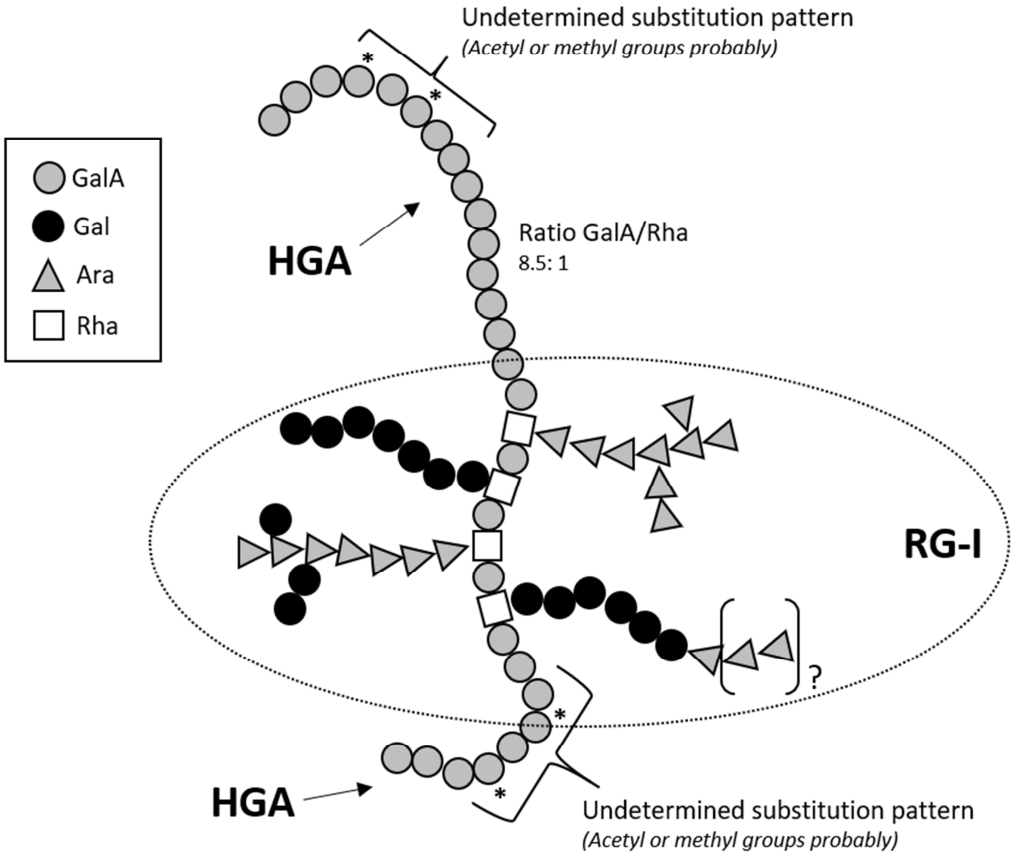

Fig. 2. Schematic representation of the hypothetical pectin primary structure determined in NRFP. HGA: Homogalacturonan, RG-I: Rhamnogalacturonan I, GalA: Galacturonic acid, Gal: Galactose, Ara: Arabinose, Rha: Rhamnose.

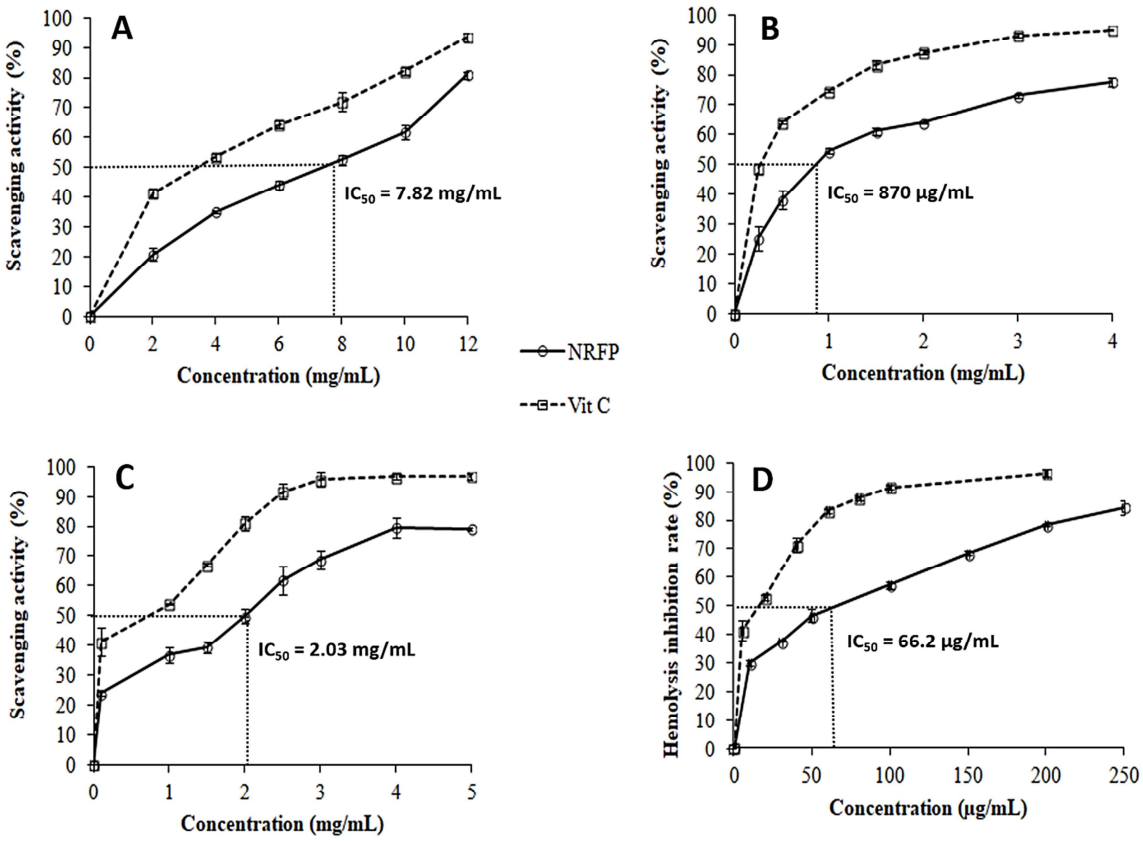

Fig. 3. *In vitro* antioxidant activity of NRFP from *Nitraria retusa* fruits. Phospho-molybdenum assay **(A)**; DPPH radical scavenging activity **(B)**; Hydrogen peroxide scavenging activity **(C)** and hemolysis inhibitory assay **(D)**. Ascorbic acid was used as a positive control.

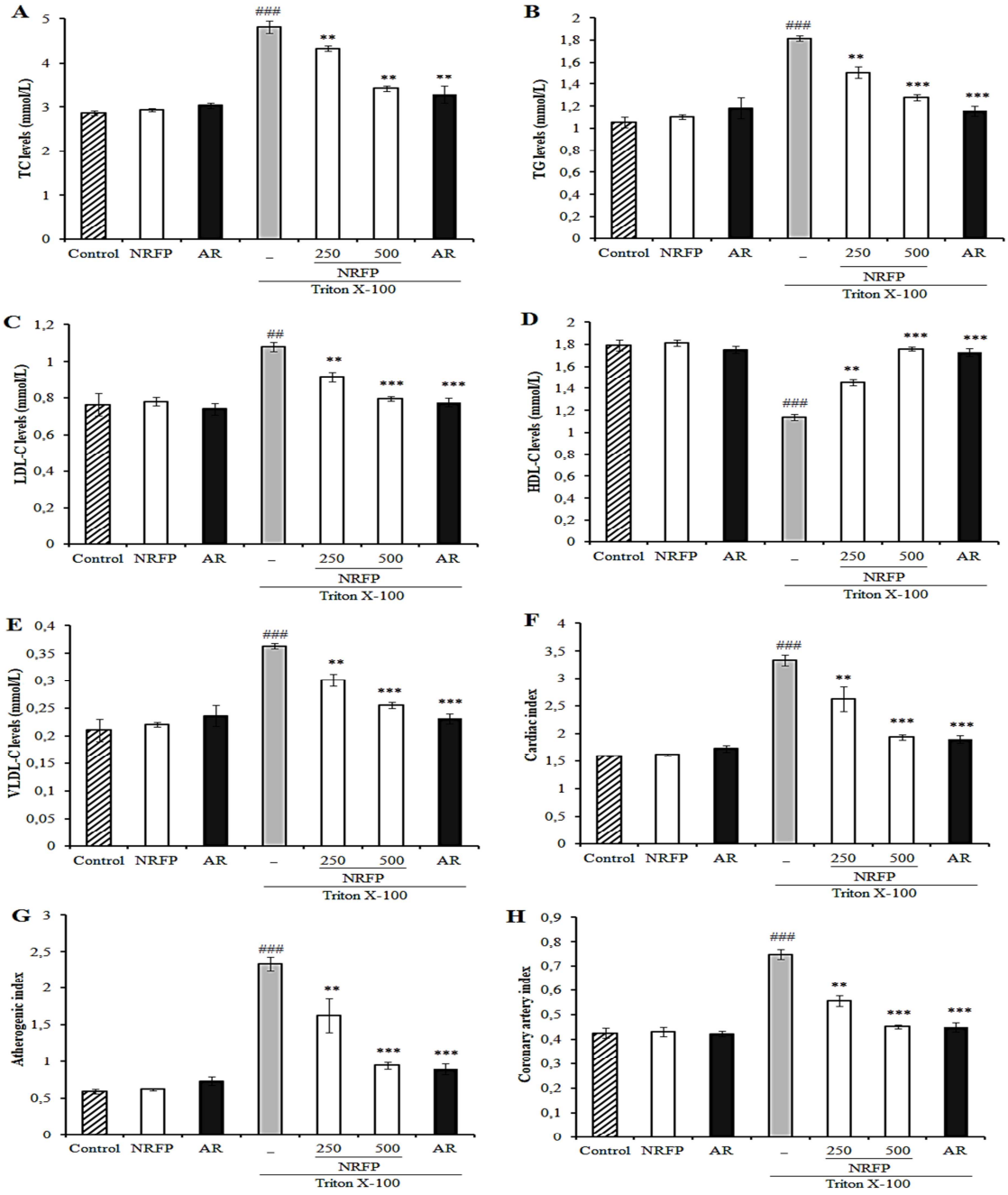

Fig. 4. *In vivo* effects of NRFP from *Nitraria retusa* fruits and atorvastatin (AR) on serum lipid profile in hyperlipidemic mice. **(A)** TC, total cholesterol; **(B)** TG, triglycerides; **(C)** HDL-C, high density lipoprotein-cholesterol; **(D)** VLDL, very low-density lipoprotein; **(E)** LDL-C, low density lipoprotein-cholesterol; **(F)** atherogenic index; **(G)** cardiac index; **(H)** coronary artery index. Values are expressed as Mean ± SEM (n = 6). ## $p < 0.01$ and ### $p < 0.001$ as compared to the normal control. ** $p < 0.01$ and ***$p < 0.001$ as compared to the hyperlipidemic mice.

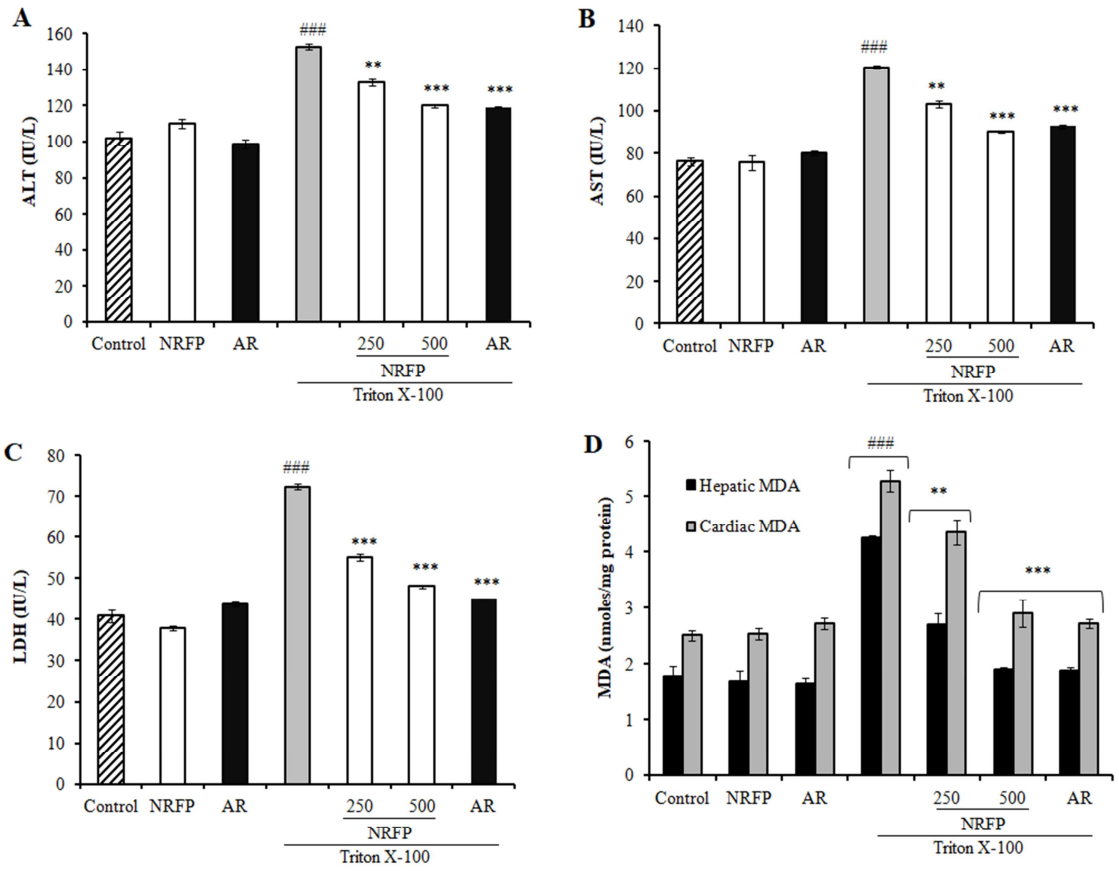

Fig. 5. *In vivo* effects of NRFP from *Nitraria retusa* fruits and atorvastatin (AR) on serum enzyme activities of **(A)** ALT, alanine aminotransferase; **(B)** AST, aspartate amino-transferase and **(C)** LDH, lactate dehydrogenase and **(D)** MDA, malondialdehyde contents in liver and heart tissues (mice model). Values are expressed as Mean ± SEM (n = 6). ### $p < 0.001$ as compared to the normal control. ** $p < 0.01$ and ***$p < 0.001$ as compared to the hyperlipidemic mice.

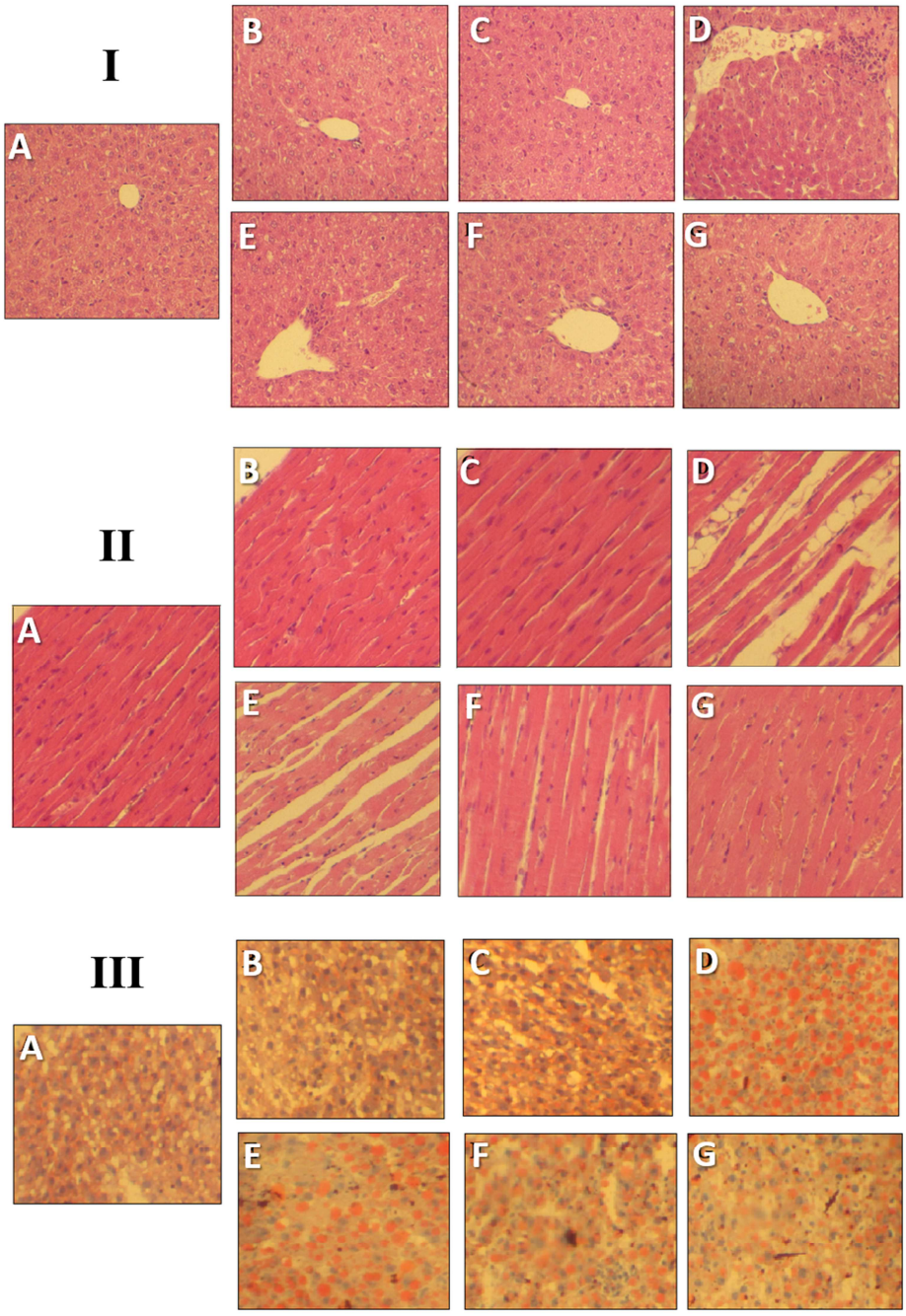

Fig. 6. Effects of NRFP from *Nitraria retusa* fruits on the liver **(I)** and cardiac tissues **(II)** of mice treated with Triton X-100 by hematoxylin–eosin at 200×. Frozen sections of hepatic tissues stained with Oil Red O **(III)**. The liver section in control group **(A)**, group fed with NRFP (500 mg/kg, b.w.) **(B)**, group treated with atorvastatin (10 mg/kg, b.w., p.o.) **(C)**, group treated with Triton-X 100 (100 mg/kg, b.w., ip) **(D)**. Liver of hypercholesterolemic mice treated with NRFP 250 and 500 mg/kg, bw **(E, F)** and hypercholesterolemic mice treated with atorvastatin **(G)**.

Table 1. Biochemical composition of NRFP from *N. retusa*.

Compositions	
Total sugar (%, w/w)	69.14 ± 0.35
Uronic acid (%, w/w)	23.14 ± 0.24
Neutral sugar (%, w/w)	46.01 ± 0.43
Starch content (%, w/w)	0.02
[NaCl] (%)	4.27
Conductivity (µs/cm)	81.80
Protein (%, w/w)	18.67 ± 0.23
Phenolic compounds (%, w/w)	5.47 ± 0.12
Organic elements (%, w/w)	
Hydrogen	1.00 ± 0.18
Nitrogen	0.21 ± 0.09
Carbon	5.03 ± 0.01

Values are means ± SD of three separate experiments.

Table 2. Macromolecular characterization and monosaccharide composition of NRFP extracted from *N. retusa* fruits.

M_w[a] (g/mol)	M_n[b] (g/mol)	PDI[c]	Monosaccharides[d] (mol%)				
			Glc	GalA	Gal	Ara	Rha
66.5 x 10^3	56.2 x 10^3	1.18	41.4	30.5	12.6	11.8	3.70

Analyses were run in duplicate and the relative standard deviations were less than 5%.

[a] M_w: Weight average molecular weight was measured by HPSEC-DRI.

[b] M_n: Number average molecular weight was measured by HPSEC-DRI.

[c] PDI: Polydispersity index M_w/M_n.

[d] Monosaccharide composition was determined by GC/MS-EI. Glc: Glucose, GalA: Galacturonic acid, Gal: Galactose, Ara: Arabinose, Rha: Rhamnose.

Table 3. Profile of partially *O*-methylated alditols acetates (PMMA) and glycosidic linkages obtained for NRFP.

Partially *O*-methylalditol acetates[a]	% [b]	Linkage type[c]	Main fragment ions (m/z)
2,3,4,6-Me_4-Gal	9.33	Gal*p*-(1→	205, 162, 161, 145, 129, 118, 102, 87, 71
2,3,6-Me_3-Gal	17.0	→4)-Gal*p*-(1→	233 162, 129, 118, 102, 99, 87, 71
MonoS[d]-Me_2-Gal	11.7	→4)-Gal*p*-(1→	–
2,6-Me_2-Gal	nd	→3,4)-Gal*p*-(1→	–
subtotal[e]	**38.0**		
2,3,4,6-Me_4-Glc	8.72	Glc*p*-(1→	205, 162, 161, 145, 129, 118, 102, 87, 71
2,4,6-Me_3-Glc	26.3	→3)-Glc*p*-(1→	234, 202, 174, 161, 129, 118, 101, 87, 71
2,4-Me_2-Glc	10.2	→3,6)-Glc*p*-(1→	305, 234, 189, 160, 139, 129, 118, 87, 74
subtotal	**45.2**		
3,4-Me_2-Rha	0.83	→2)-Rha*p*-(1→	175, 162, 131, 118, 102, 89, 72
3-Me-Rha	3.65	→2,4)-Rha*p*-(1→	203, 190, 143, 130, 101, 88, 74
subtotal	**4.48**		
2,3,5-Me_3-Ara	1.33	Ara*f*-(1→	162, 161, 145, 129, 118, 102, 101, 87, 71
2,3-Me_2-Ara	8.02	→5)-Ara*f*-(1→	189, 129, 118, 102, 87, 71
2-Me-Ara	2.94	→3,5)-Ara*f*-(1→	261, 127, 118, 99, 85
3-Me-Ara	nd	→2,5)-Ara*f*-(1→	190, 189, 130, 129, 88, 87
subtotal	**12.3**		

All analyses were run in duplicate and the relative standard deviations were less than 5%.

[a] 2,4,6-Me_3-Glc=2,4,6-tri-*O*-methyl-glucitol-acetate, etc.

[b] % of peak area of *O*-methylated alditol acetates relative to total area, determined by GC–MS.

[c] Based on derived *O*-methylalditol acetates.

[d] Residues were monosubstituted by a non-defined group.

[e] Corresponded both for Gal*p* and Gal*p*A